European Review for Medical and Pharmacological Sciences 2022; 26: 9393-9408

Multiple targets of Nrf 2 inhibitor; trigonelline in combating urethane-induced lung cancer by caspase-executioner apoptosis, cGMP and limitation of cyclin D1 and Bcl2

M.A. HAMZAWY[1], A.M. ABO-YOUSSEF[2], M.N. MALAK[2], M.M. KHALAF[2]

[1]Pharmacology and Toxicology Department, Faculty of Pharmacy, Fayoum University, Fayoum, Egypt
[2]Pharmacology and Toxicology Department, Faculty of Pharmacy, Beni-Suef University, Beni-Suef, Egypt

Abstract. – OBJECTIVE: Among other types of cancerous lesions, lung cancer is one of the prevalent causes of death. Trigonelline is a plant alkaloid, a significant constituent in coffee, and has shown health benefits in several disorders. The present study aims to investigate the potential therapeutic role of trigonelline in lung cancer.

MATERIALS AND METHODS: Seventy-five BALB/C mice were assigned to five groups and treated for 150 days as follows (1): normal control group; (2) trigonelline only (50 mg/kg/ P.O) daily for the last thirty days; (3) urethane (1.5 g/kg B.w/i.p) at day one and sixty; (4) urethane and carboplatin (15 mg/kg i.p) for the last thirty days; and (5) urethane and trigonelline for the last thirty days. Tumor size was measured while blood and lung were collected for biochemical, western blotting analysis, and histological examinations.

RESULTS: Urethane demonstrated significant changes in all biochemical and molecular parameters and histological examinations. In animals pretreated with urethane, trigonelline significantly reduced tumor size and restored Nrf2, NF-κB p65, Bcl-2, Cyclin D1, ICAM-1, and MMP-2, along with improving cGMP and active caspase three and refining histological architectures.

CONCLUSIONS: Nrf2 signaling may be a promising therapeutic target for adenocarcinoma protection or management. Due to its multiple therapeutic effects on Nrf2, cyclin D1, NF-κB pathways, and the BAX/Bcl2 axis, trigonelline significantly induced cell cycle arrest and apoptosis.

Key Words:
Lung cancer, Nrf 2, Trigonelline, BALB/C, Apoptosis, Cyclin D1.

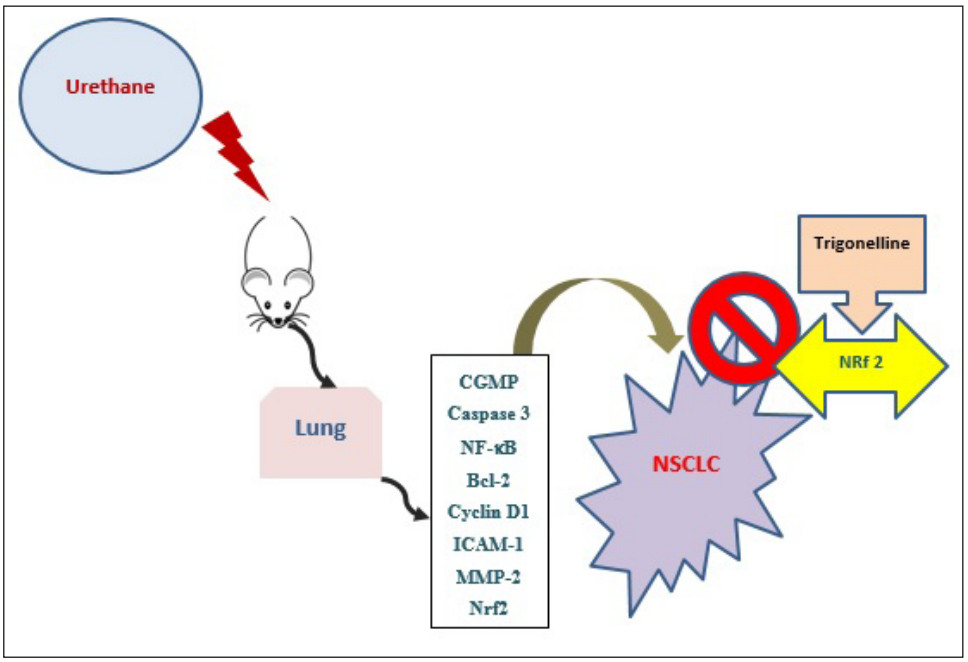

Graphical_Abstract. Multiple targets of trigonelin in urethane-induced lung cancer.

Corresponding Author: Mohamed A. Hamzawy, MD; e-mail: mam43@fayoum.edu.eg

Abbreviations

CYFRA 21-1: Cytokeratin 19 fragments; IGF-1: Insulin-like growth factor-1; cGMP: Cyclic guanosine monophosphate; Bcl-2: B-cell lymphoma 2; ICAM-1; Intercellular Adhesion Molecule 1; MMP-2: Matrix metalloproteinase-2; NF-κB: Nuclear factor kappa light chain enhancer of activated B cells; Nrf2; Nuclear factor erythroid-2 related factor 2.

Introduction

Lung cancer is a major public health concern representing a leading cause of mortality worldwide[1,2]. Lung cancer is considered the primary type of cancer that triggers death in males, while breast cancer is the leading cause of death in females[3]. Patients diagnosed with a lung cancer account for 11.4% of cancerous patients, as well as 19% of worldwide death[1,4]. In 2020, 2.2 million new lung cancer cases and 1.8 million lung cancer deaths were globally reported, including 230,000 cases and 132,000 deaths in the United States[3,5,6]. According to the National Population-Based Registry Program in Egypt (NCRPE), lung cancer is one of the most common five types of cancer (breast, brain, liver, and urinary bladder)[7,8], and it is frequently diagnosed as adenocarcinoma[3]. In 2020, 6,538 (4,851 male patients and 1,687 female patients) were newly diagnosed with cancer in Egypt[3].

Globally, lung cancer has risen to the top of the list of cancer-related deaths, accounting for approximately 19% of all cancer deaths annually, indicating a significantly increased incidence[9]. There are two types of lung cancer, small cell lung cancer (SCLC) and non-small cell lung cancer (NSCLC)[10]. NSCLC represented 80% of lung cancer cases and was sub-classified into several subclasses of carcinomas, followed by SCLC[11]. Among the different NSCLC subtypes, adenocarcinoma is the most commonly found type in Egypt, accounting for 40% of all NSCLC cases[7,8].

According to the type and stage of lung cancer, therapeutic modalities are selected as chemotherapy, surgery, radiotherapy, and recently targeted immune-based therapy[12]. However, platinum-based chemotherapy (cisplatin or carboplatin) was previously described as the first-line treatment for lung cancer[13]. Currently, incorporating immunotherapy (pembrolizumab or atezolizumab) into chemotherapy has synergetic effects[14] in overcoming numerous challenges in conventional chemotherapy, like acquired drug resistance and adverse drug reactions[15].

The nuclear factor erythroid 2-related factor 2 (Nrf2) plays a vital role in maintaining cellular hemostasis and proliferation[16]. The Kelch-like ECH-associated protein 1 (Keap1) pathway degrades Nrf2 regularly *via* the proteasome pathway. Additionally, oxidative stress and cellular disruption of the Keap1 pathway are associated with stagnation and accumulation of Nrf2. It may bind to the antioxidant response element (ARE) sequences which is a target gene regulator in Thioredoxin reductase 1 (Txnrd1), glutamate-cysteine ligase, Peroxiredoxin 1 (Prdx1), Nicotinamide adenine dinucleotide dehydrogenase; NAD(P)H, and Glutathione S-transferase (Gst)[17]. Therefore, the Nrf2-Keap1 signaling pathway protects cells against free radicals and reactive oxygen species[18]. Moreover, the Nrf2-Keap1 is responsible for encoding antioxidants and detoxification enzymes through a redox sensing system[19].

Nrf2 plays a dual role on both sides, a tumor suppressor on the good side but an oncogenic agent on the dark side[20]. Consequently, Nrf2 meets the criteria for being investigated in cancer research and cellular hemostasis. The persistent activation of Nrf2 provides a long-term existence for cancer cells against apoptosis and reactive oxygen species (ROS)[21]. Interestingly, high expression of Nrf2 may be linked to poor prognosis of lung, prostate, and breast cancers[22].

In the same context, the pro-oncogenic function of Nrf2 has been reported to determine the potential effect of Nrf2 inhibition in cancer treatment with further explanation to develop novel therapeutic modalities for lung cancer[23]. Consequently, prior studies highlighted the biological role of Nrf2 with other therapeutic targets that may contribute to developing novel strategies for lung cancer diagnosis and treatment[23].

Researchers were particularly interested in studying the potential role of trigonelline in disease prevention among natural products and herbs[24]. Trigonelline, the main constituent in coffee, is an alkaloid that has anti-inflammatory, antioxidant, anti-microbial, and anti-hyperglycemic effects[25,26]. Trigonelline is a potent inhibitor of Nrf2 transcription by interfering with the nuclear translocation of Nrf2 and blocking Nrf2-dependent proteasome activity[27]. Previous reports demonstrated that trigonelline has antitumor activity against hepatic and colon cancer cells by inhibiting ROS-mediated cancer cell invasiveness[28]. Trigonelline makes pancreatic and colon more susceptible to chemotherapy and improves cholangiocarcinoma response to cisplatin treatment[22,27,29]. Furthermore, due to Nrf2 suppres-

sion, trigonelline (TG) has a synergistic effect with anticancer drugs such as buthionine sulfoximine (BSO), and auranofin (Aur), and artesunate in head and neck cancer cells[30,31]. These findings prompted us to investigate the therapeutic activity of trigonelline in the BALB/C model of non-small lung cancer (NSCLC).

Materials and Methods

Animals

BALB/C male mice weighing 25-30 g were purchased from a laboratory animal facility – Pharmacology, and Chemistry Research Center (PCRC) – Misr University for Sciences and Technology Park, Six October City, Egypt. Animals were kept in a fully transparent polycarbonate filter top for mice in a room with proper control of room temperature (25 ± 1ºC), contamination, and illumination (12 h dark/light cycle) at the Laboratory Animal House, Faculty of Pharmacy, Beni-Suef University. Mice were fed laboratory diet pellets and water *ad libitum*. Mice were left for a week to acclimate. The current study's procedures were reviewed and approved by the institutional animal care and use committee (IACUC), Beni-Suef University, and followed the guidelines of Laboratory Animals Guidance for Care and Use (National Institutes of Health, publication no. 85-23, revised 1985). All techniques were performed by gently handling experimental animals with no necessary stress, pinching, and pressure.

Materials

Urethane (ethyl carbamate) and trigonelline were purchased from Sigma Chemical Company (St. Louis, MO, USA), and dissolved in saline and distilled water. Carboplatin was purchased as carboplatin 150 mg/15ml vial (Mylan, Canonsburg, PA, USA) and dissolved in 0.9% saline (NaCl). Ketamine and xylazine were gifted from SIGMA TEC Pharmaceutical industries (Cairo, Egypt), and Adwia Pharmaceuticals Co., 10th of Ramadan City (Cairo, Egypt), respectively.

Ethanol, xylene, paraffin wax, and formaldehyde were purchased from EL Nasr Pharmaceutical Company, (Cairo, Egypt). Cytokeratin 19 fragments (CYFRA21-1) kit was purchased from Genorise Scientific, (Inc, Berwyn, PA, USA), while the Insulin-like growth factor-1 (IGF-1) reagent kit was obtained from Alpco Diagnostics, (Salem, NH, USA). B-cell lymphoma 2 (Bcl-2), cyclin D1, cyclic guanosine monophosphate (cGMP), intercellular adhesion molecule 1 (ICAM-1), and matrix metalloproteinase-2 (MMP-2) reagent kits were purchased from MyBioSource, (San Diego, CA, USA). Nrf2, active caspase 3, and nuclear factor kappa light chain enhancer of activated B cells (NF-κB p65) primary antibodies for western blotting assay were procured from Thermo Fisher Scientific, (Waltham, MA, USA). A horseradish peroxidase (HRP)-conjugated secondary antibody was purchased from Novus Biologicals, (Littleton, CO, USA). Other chemicals and reagents in the high analytical grade were purchased from certified suppliers.

Experimental Design

As demonstrated in Figure 1, BALB/C mice were randomly distributed into five groups (n=15/group) after one week of acclimatization by a technical assistant who was not engaged in the subsequent work:

- Group I: Untreated normal control.
- Group II: Animals treated with trigonelline (50 mg/kg, P.O) every day for the last thirty days[30].
- Group III: Animals were treated with two successive doses of urethane (1.5 g/kg i.p) on urethane on the first day and day sixty of the study period.
- Group IV: Animals treated with urethane and carboplatin (15 mg/kg i.p) every other day for the last thirty days[32].
- Group V: Animals treated with urethane and trigonelline (50 mg/kg, P.O) for the last thirty days.

Mice fasted overnight on day 150 (the end of the treatment period), and blood was withdrawn from the retro-orbital vein using non-heparinized micro-hematocrit capillary tubes after peritoneal injection of ketamine (12.5 mg/kg) and xylazine (1.5 mg/kg) for anesthesia[33]. The serum was obtained from the collected blood by centrifugation at 3000 × g for 20 minutes. Serum was stored at -20°C refrigerators until cytokeratin 19 fragments (CYFRA21-1) and insulin-like growth factor 1(IGF-1) were measured. Afterward, mice were euthanized under light anesthesia, and then, their lungs were rapidly removed. The size of the lung tumor was measured utilizing a caliper. Each lung was divided into three parts. The first part was assigned for histological examinations after fixation in 10% formalin, and the second part was sampled to obtain 20% w/v homogenate after homogenization for 0.05-0.1 g of lung tissue in phosphate buffer (PH 7.4). The homogenate was then centrifuged at 1700 × g for 10 minutes using a cooling centrifuge (4°C). Subsequently, the su-

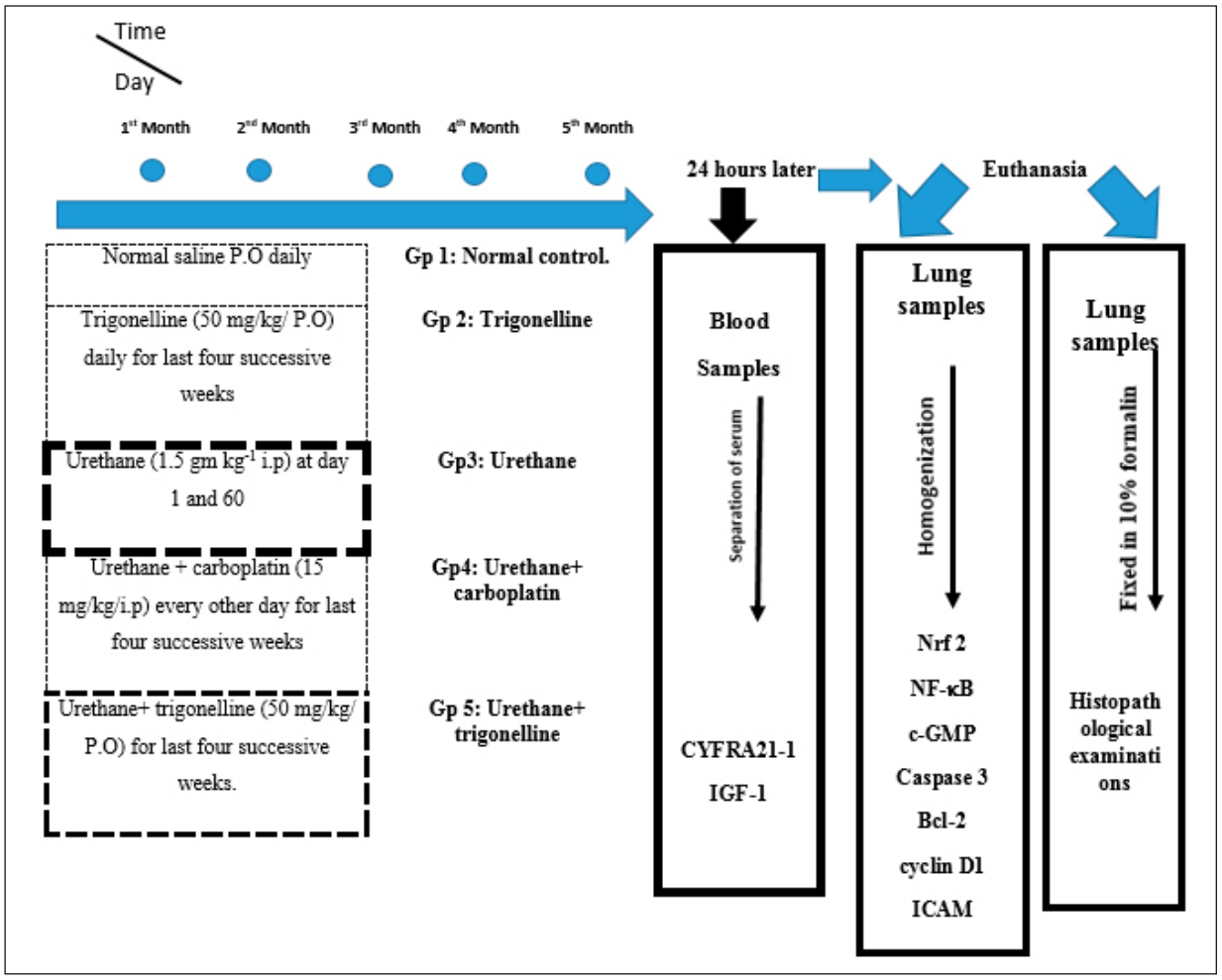

Figure 1. Experimental design representing the allocation of mice in different treatment groups. Mice were received and treated according to assigned groups for 5 months. 24-hour post-last exposure blood samples were collected for biochemical investigations in serum then the mice were mercy killed and lung were isolated for molecular evaluations and histopathological examination.

pernatant was kept at -80°C until measurement of cyclic guanosine monophosphate (cGMP), B-cell lymphoma 2 (Bcl-2), cyclin D1, intercellular adhesion molecule-1 (ICAM-1), and matrix metalloproteinase-2 (MMP-2). The remaining part was subjected to a western blotting assay to determine the expression of active caspase 3, nuclear factor kappa light chain enhancer of activated B cells (NF-κB p65), and Nrf2. During the sample analysis of all previous independent studies, where an independent investigator performed sample coding and decoding, the researchers were blinded to the identity of the samples.

BALB/C Model for NSCLC

NSCLC was experimentally developed after urethane treatment (1.5 g/kg, i.p.) on two different occasions. The first dose was administered on day one and the second on day sixty of the 150 days of the study period[34].

Calculation of Lung Tumor Volumes

The following formula was utilized to calculate lung tumor volumes, as previously prescribed[35,36]:

- Volume (mm^3) = (l x w^2) / 2
- l (length): the longest diameter
- w (width) is the diameter perpendicular to the length.

Biochemical Parameters in Serum Samples

CYFRA 21-1 and IGF-1 were assessed using Enzyme-Linked Immunosorbent Assay (ELISA) kits. CYFRA 21-1 was determined as previously

described[37,38], while IGF-1 was measured according to the previously described method[39,40].

Determination Biomarkers in Lung Homogenate Samples

cGMP content was measured using an ELISA technique[41].

Determination of Apoptotic Activity

According to the product information[42,43], the anti-apoptotic marker contents (Bcl-2 and cyclin D1) were measured using ELISA kits[42,43]. The standard working solutions, samples (tissue homogenate), and the control were added two times to the plate wells and incubated for 90 min at 37°C. The biotinylated antibody was then added the plate was incubated at 37°C. Before adding the Avidin-Horseradish, wash three times with the washing buffer. Before 30 minutes of incubation at 37°C, peroxidase enzyme conjugate (HRP conjugate substrate) was added. Afterward, the plate was washed five times before the addition substrate solution. The plate was incubated for 15 min at 37°C in a dark place. Finally, the reaction was stopped with a pipette before measuring at 450 nm.

MMP-2 and ICAM-1 Content

The detection of MMP-2 and ICAM-1 biomarkers were carried out by ELISA techniques as previously described methods[44,45].

Western Blot Assay of Nrf2, NF-κ B p65, and Active Caspase 3

Sodium Dodecyl Sulfate-Poly Acrylamide Gel Electrophoresis was used to separate 50 g protein from lung tissues (SDS-PAGE). On the nitrocellulose membrane, western blotting was used to detect antibodies. The membrane was kept overnight at 4°C with diluted primary antibodies of NF-kB p65, Nrf2, and active caspase 3 with TBST (1:2000) and kept overnight with the membrane. Second incubation was performed at room temperature with horseradish peroxidase (HRP)-conjugated secondary solution for one hour. Before and after incubation, the membrane was washed twice with TBST. A secondary fluorescent antibody (BIO-RAD, Hercules, CA, USA) was used for signal detection. A CCD camera-based imager was used to determine the band intensity. The band intensity of protein expression was measured and compared to the control using Bio-Rad image analysis software after normalization with beta-actin. Each experiment was repeated at least three times.

Histological Examinations

A few millimeters from lung tissues were excised from 3 to 5 mice randomly selected from each group and processed for histological studies. In brief, fixation in 10% formalin for 48 hours is followed by complete washing with water for one hour and dehydration with ethanol with serial dilution by water before purification of the sample by xylene and embedding in paraffin wax. For histological studies, slicing sections (5-6 m) were stained with Hematoxylin and Eosin stain (H&E)[46].

Statistical Analysis

The data and statistical analysis were carried out following the recommendations for experimental design and analysis in pharmacology[47]. Data were expressed as the mean ± standard error of the mean using the SPSS program version 22 (IBM Corp. Armonk, NY, USA). The mean differences between groups were determined using one-way analysis of variance (ANOVA), followed by Tukey-Kramer multiple comparisons at a significance level of $p < 0.05$[48].

Results

Tumor Incidence and Volume

Eighty percent (n=15) of urethane-treated mice developed cancerous lesions. Carboplatin or trigonelline decreased the incidence to 26.67% and 40.00%, respectively.

Tumor volume was significantly increased in mice treated with two successive doses of urethane, as shown graphically in Figure 2. Tumor volume and size were significantly reduced in mice treated with trigonelline and urethane.

Bodyweight of BALB/C Mice

Trigonelline treatment resulted in a 7.08% weight gain, while urethane treatment decreased body weight by about 8.60%. Interestingly, urethane and carboplatin treatment exhibited a 2.60% reduction in body weight. In urethane-treated animals, trigonelline induced a 3.83% weight gain (Table I).

Lung Cancer Prognosis Biomarkers and cGMP Content

According to Figure 3 (A, B), trigonelline showed no significant difference from the control group. Animals treated with urethane had elevated CYFRA 21-1 and IGF-1 levels compared to

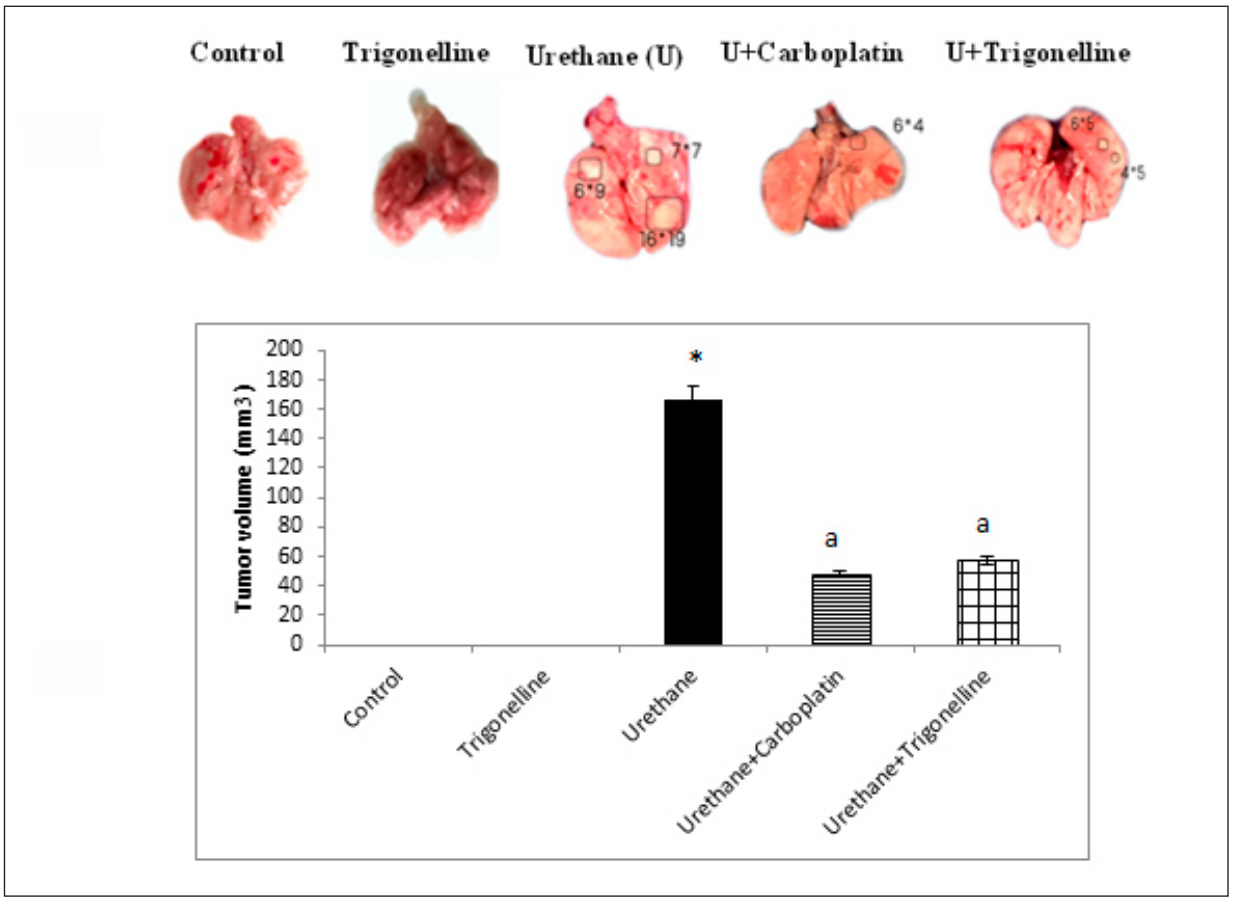

Figure 2. Effect of different treatments on tumor incidence and volume. Values were expressed as mean ± S.E.M of 15 mice per group. Statistical analysis were performed by One-way ANOVA followed by Tukey-Kramer multiple comparisons test. * Significantly different from normal control at $p < 0.05$. [a] Significantly different from urethane at $p < 0.05$.

the untreated control group. Compared to urethane-treated mice, carboplatin or trigonelline treatment showed a substantial decrease in CYFRA 21-1 and IGF-1 levels. Trigonelline restores CYFRA 21-1 and IGF-1 levels comparable to the control group. As demonstrated in Figure 3 (C), animals treated with trigonelline in combination with urethane showed a significant improvement in cGMP lung content more than the control group.

Table I. Effect of trigonelline on the body weight of BALB/c mice treated with urethane-induced lung cancer.

Groups/ Weight (g)	Normal control	Trigonelline	Urethane	Urethane + carboplatin	Urethane + trigonelline
Before treatments (at the end of induction period, 120 days)	35.00 ± 0.21	34.65 ± 0.25	32.50 ± 0.06*	33.02 ± 0.11*	32.60 ± 0.09*
At the end of treatments period (30 days)	37.88 ± 0.62	37.29 ± 0.12	29.70 ± 0.15*	32.16 ± 0.23*a	33.90 ± 0.22*a
% of weight gain after treatment	7.60%	7.08%	—	—	3.83%
% of weight inhibition after treatment	—	—	8.60%	2.60%	

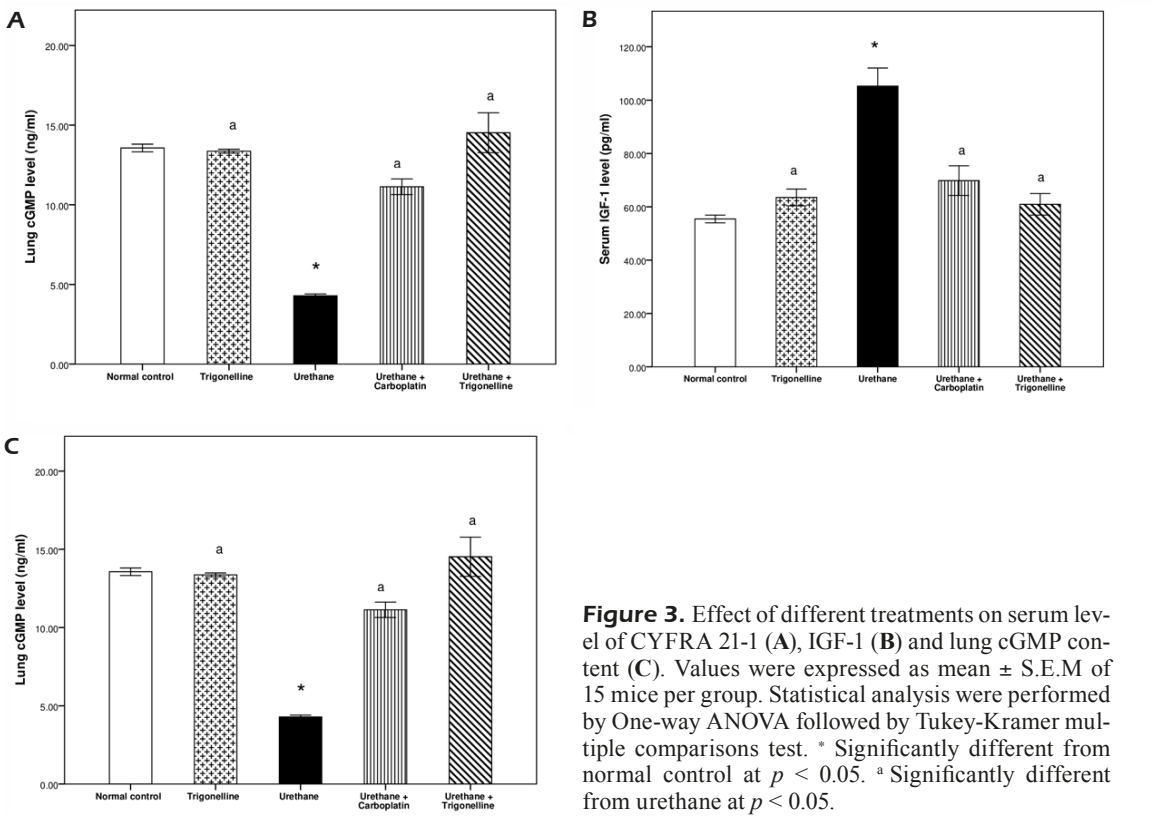

Figure 3. Effect of different treatments on serum level of CYFRA 21-1 (**A**), IGF-1 (**B**) and lung cGMP content (**C**). Values were expressed as mean ± S.E.M of 15 mice per group. Statistical analysis were performed by One-way ANOVA followed by Tukey-Kramer multiple comparisons test. * Significantly different from normal control at $p < 0.05$. [a] Significantly different from urethane at $p < 0.05$.

Apoptotic Biomarkers

The effect of trigonelline and carboplatin on the lung contents of Bcl-2 and cyclin D1 is graphically demonstrated in figures 4A and 4B. Animals treated with urethane showed a significant increase in Bcl-2 and cyclin D1 levels. Animals treated with trigonelline after urethane restored Bcl-2 and cyclin D1 to the same levels as the control group.

ICAM-1 and MMP-2 Lung Content

As shown in Figure 5 (A, B), the present study's findings indicated that urethane treatment resulted in the elevation of ICAM-1 and MMP-2 contents compared to the normal control. Trigonelline or carboplatin attenuated the severe changes in ICAM-1 and MMP-2 levels in animals treated with urethane only. However, trigonelline treatment showed a substantial reduction of ICAM-1

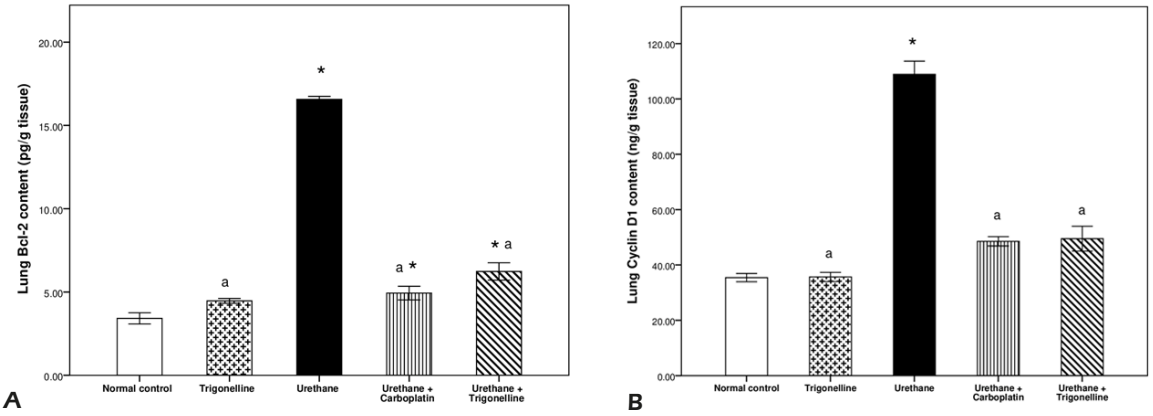

Figure 4. Effect of different treatments on lung content of Bcl-2 (**A**) and Cyclin D1 (**B**). Values were expressed as mean ± S.E.M of 15 mice per group. Statistical analysis were performed by One-way ANOVA followed by Tukey-Kramer multiple comparisons test. *Significantly different from normal control at $p < 0.05$. [a]Significantly different from urethane at $p < 0.05$.

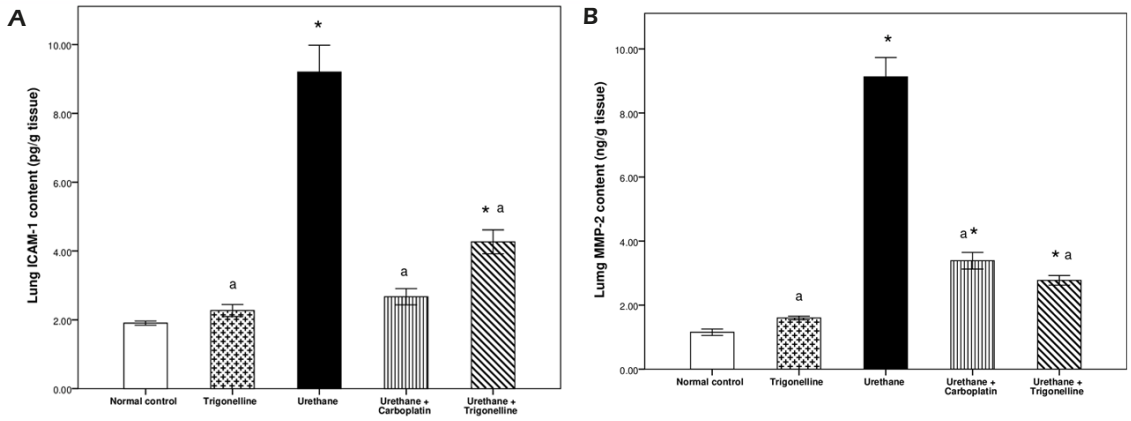

Figure 5. Effect of different treatments on lung content of ICAM-1 (**A**) and MMP-2 (**B**). Values were expressed as mean ± S.E.M of 15 mice per group. Statistical analysis were performed by One-way ANOVA followed by Tukey-Kramer multiple comparisons test. *Significantly different from normal control at $p < 0.05$. [a]Significantly different from urethane at $p < 0.05$.

and MMP-2 levels by almost 75% compared to animals treated with urethane only.

Protein Expression of NF-κ B p65, Active Caspase 3, and Nrf2

To investigate trigonelline's antitumor activity, the protein expression of NF-κB p65, active caspase 3, and Nrf2 were evaluated by western blotting assay. As shown in figure 6 (A, B, C, D), the current study results showed that protein expression of NF-kB and Nrf2 were significantly increased in the urethane treated group while the successive treatment with trigonelline or carboplatin reduced their expression. Trigonelline demonstrated a pronounced improvement in NF-kB p65 and Nrf2 levels in mice pretreated with urethane.

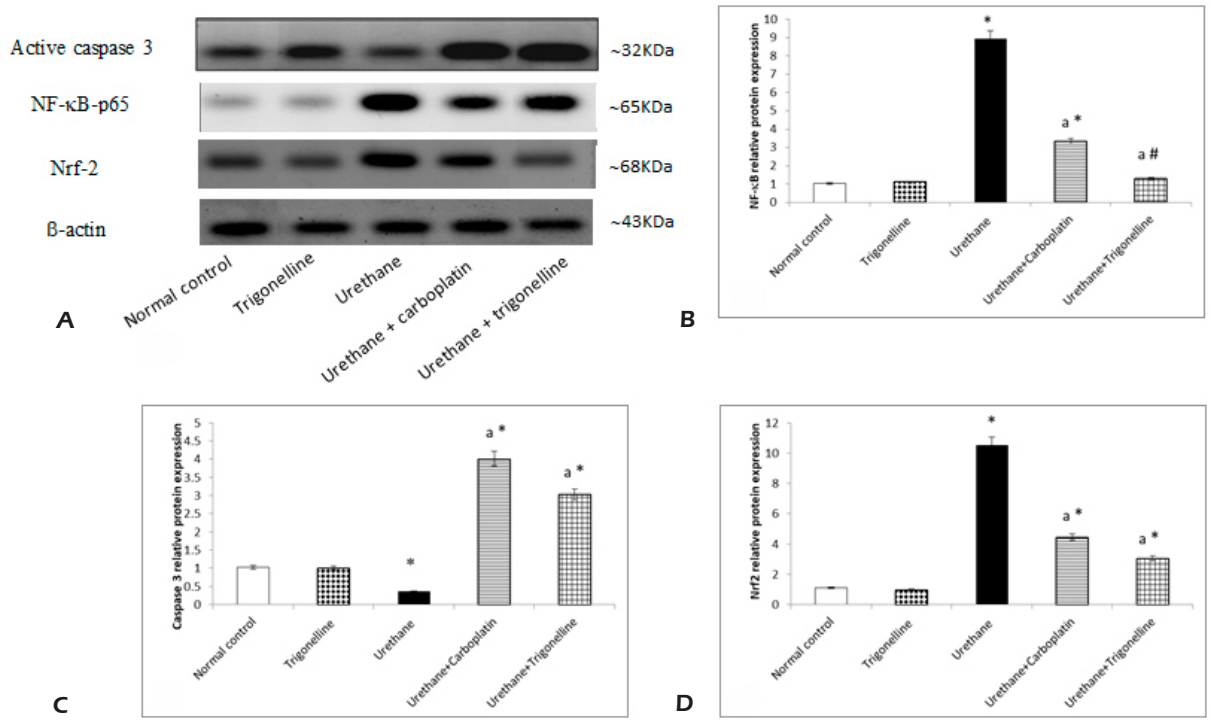

Figure 6. Variation on protein expressions of lung (**A**), NF-kB (**B**), Caspase 3 (**C**) and Nrf2 (**D**) in different treated groups. Values were expressed as mean ± S.E.M of 15 mice per group. Statistical analysis were performed by One-way ANOVA followed by Tukey-Kramer multiple comparisons test. *Significantly different from normal control at $p < 0.05$. [a]Significantly different from urethane at $p < 0.05$.

On the contrary, there was a remarked reduction in active caspase 3 levels in mice treated with urethane.

Additionally, active caspase 3 level was significantly elevated in mice treated with either trigonelline or carboplatin after urethane treatment, more or less like the control group itself. There is an evident improvement in animals treated with trigonelline.

Histopathological Studies

As demonstrated in Figure 7, the examination of lung sections from the untreated control group had a normal pattern of bronchi, alveoli structure, and normal vasculatures without any signs of any tumor cells (Figure 7A). The photomicrographs revealed no significant change in the lung tissues in mice treated with trigonelline (Figure 7B). In contrast, urethane treatment exhibited masses of

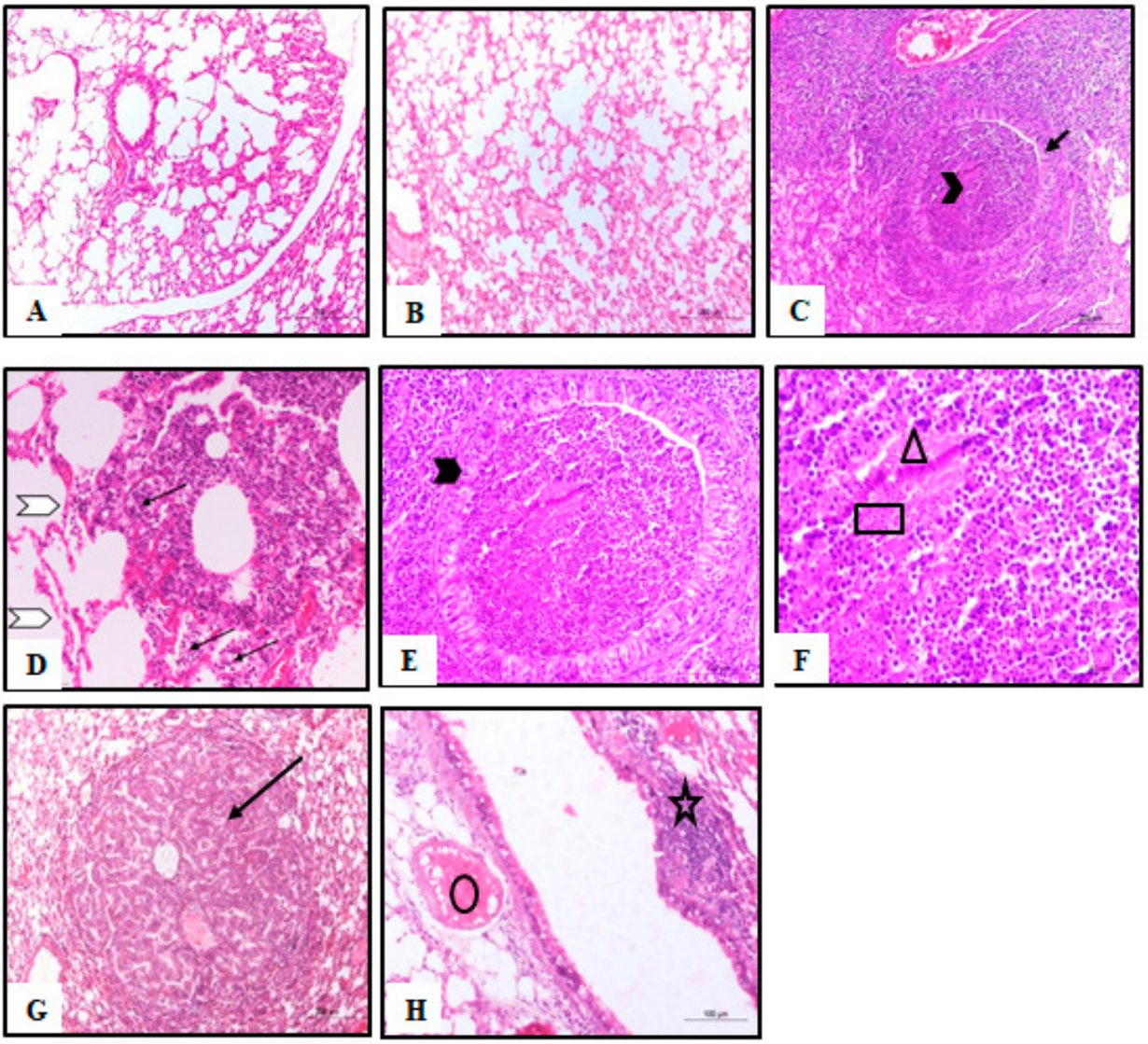

Figure 7. Effect of different treatments on histological architectures of lung. **A,** Lung section from control group with normal alveoli and vasculatures (H&E X100). **B,** Lung section of trigonelline group showing nearly normal bronchi and bronchioles (H&E X100). **C-D,** Lung sections of the urethane group showing intrabronchial and peribronchial neoplastic along with aggregations of tumor cells around the bronchioles with compensatory edema and congestion of vasculature (H&E X200). **E-F,** Higher magnification microphotographs of urethane treated group presenting characteristic mitotic features, polymorphism and necrosis of tumor cells besides the replacement of bronchus epithelium cells with tumor cells (H&E X200), (H&E X400). **G,** Mice treated with carboplatin after urethane showing incomplete recovery with normal vasculatures (H&E X100). **H,** Treatment with trigonelline after urethane showing mononuclear cells aggregations with congestion of the blood vessels with no tumor cells (H&E X 200).

tumor cells around the bronchioles with polymorphism and advanced mitotic features, whereas urethane treatment exhibited masses of tumor cells around the bronchioles with polymorphism and advanced mitotic features. The epithelium cells of the bronchus were replaced by neoplastic cells (arrow), and the lumen was fully occupied with tumor cells (arrowhead) (Figure 7C). In addition, dilated alveoli with compensatory emphysema in some areas (arrowhead), interalveolar infiltration with neoplastic cells (arrow), and interalveolar capillary congestion were observed in lung sections from the urethane-treated group (Figure 7D). A higher magnification section of the bronchus revealed pseudostratified columnar epithelium cells that were partially replaced by neoplastic cells (arrowhead) (Figure 7E). Another magnification of the previous slide presented in Figure 7F revealed distinct malignant features of peribronchial (P) neoplastic cell aggregations (circle) with focal necrosis (triangle) and karyorrhexis (square).

Carboplatin and urethane treatment showed few focal areas of adenocarcinoma (thin arrow), indicating incomplete recovery, and the rest of the lung sections appeared normal in structure with normal alveoli and bronchioles (thick arrow) (Figure 7G). Photomicrographs from the lung of trigonelline and urethane treated mice demonstrated a focal peribronchial area of mononuclear cell aggregations with congestion of the blood vessels with no tumor cells or hyperplasia in the bronchial epithelium cells (Figure 7H). The histopathological alterations in the lung were graded for all groups and presented in Table II.

Discussion

There are dynamic challenges opposing the development of efficient and safe therapeutic modalities for lung cancer treatment. Due to acquired drug resistance and cancer heterogenicity, the use of conventional chemotherapy is generally limited. Therefore, finding an effective therapeutic regimen with a novel biological mechanism for lung cancer gained great attention. Therefore, we are encouraged to study the potential effect of trigonelline on lung tumorgenesis induced by urethane in BALB/C mice.

The study outcomes of the present work revealed that urethane increased the size of the tumor incidence and volume. Similar to the current results, Chen et al[49] reported that urethane induced tumor multiplicity[49]. In the same context, urethane showed a significant loss of body weight in mice, which may be attributed to tumor severity induced by chemical carcinogen[50]. The present study found that the link between lung adenocarcinoma and urethane treatment was confirmed by a significant increase in IGF-1 and CYFRA 21-1 levels. CYFRA 21-1 is a prognostic biomarker for NSCLC, a predictor for patient response to therapeutic interventions, and an indicator for a poor prognosis and worsening survival of NSCLC[51]. IGF-1 plays a vital role in cellular proliferation, differentiation, and apoptosis in several types of cancer as lung cancer[52]. In addition, IGF-1 is a promising predictive tool for the patient's response when treated with chemotherapy[53]. In recent years, mounting evidence showed that IGF-1 plays an essential role in promoting the survival of tumor cells, protection against apoptosis, enhancement of cell growth, and proliferation[54]. IGF-1 has also been reported to induce lung cancer by inducing ETS Like-1 protein (ELK1) and mitogen-activated protein kinase (MAPK)[55].

cGMP is a member of the cGMP/ Protein Kinase G (PKG) cascade for the apoptotic pathway, which is a potential therapeutic target for various types of cancer. Animals treated with urethanes exhibited a significant reduction of cGMP content of lung homogenate. The reduction in cGMP may

Table II. Histopathological effect of different treatments on the lung.

Histopathologic alterations in lung	Normal control	Trigonelline	Urethane	Urethane + carboplatin	Urethane + trigonelline
Aggregations of tumor cells	–	–	+++	++	–
Advanced mitotic features	–	–	+++	+	–
Neoplastic cells	–	–	+++	++	–
Neoplastic cell aggregations	–	–	+++	++	–
Congestion of the vasculatures	–	–	+++	++	+

Absent - Mild + Moderate ++ Sever +++

be due to the depletion of antioxidative enzymes through its active metabolites (vinyl carbamate). Vinyl carbamate is a potent mutagen and electrophilic species promotor. Therefore, lung antioxidant capacity alteration indicated to the impairment of cGMP-dependent protein kinase[25,34].

The current study found that urethane treatment is associated with cellular proliferation, inflammation, and invasion[56] indicated by elevation of NF-κB p65[57]. NF-kB plays a central role in anti-apoptotic Bcl-2 and cyclin D1 expression activation. They keep advanced cellular protection against a cytotoxic activity of chemotherapy[58] with a rapid cell transition from G1 to S phase[59]. In addition, NF-κB contributes to enhancing MMP2 expression and ICAM-1 induction[60,61].

The carcinogenic effect of urethane can be proved by significantly reducing active caspase 3 expressions, which is widely reported in an apoptosis through the cleavage of poly ADP-ribose polymerase (PARP), causing DNA fragmentation[62]. This conclusion is consistent with a previous research that affirmed urethane treatment is associated with caspase 3 inhibition and down-regulation of pro-apoptotic proteins Bcl-2-associated X protein (Bax)[63]. The disagreement with earlier studies may be due to a difference in the duration from urethane exposure to study termination[64]. In the same context, urethane treatment demonstrated significantly elevated Nrf2 expression in mice, which was associated with cancer progression and advanced lung cancer progression[65,66]. Activation of Nrf2 expression has previously been linked to lung tumorigenesis in urethane treatment[67]. The Nrf2-Keap1 pathway has a dual role; the first is a defensive role by cellular hemostasis preservation[68]. Nrf2 is regulated by the interaction of Nrf2 with the cytosolic repressor protein; Keap1[23] prevents the initiation of a cancerous lesion. The second role is affirmed nearly by a prior study that exhibits Nrf2 as a promoter for cancer cell progression with resistance to chemotherapy[69].

Carboplatin is a standard therapy in NSCLC. The use of carboplatin is limited by chemoresistance that acquired from cancer cells and hematological toxicities[70]. Carboplatin induces cytotoxicity by forming DNA adducts at N7 positions of adenine and guanine in DNA[71]. Carboplatin's antitumor activity in lung adenocarcinoma was confirmed by lowering IGF-1 and CYFRA 21-1 serum levels[72]. However, the current study revealed that carboplatin treatment was substantially improved in all molecular, biochemical, and histological studies. These findings are consistent with previous research work that showed that carboplatin induced reduced glutathione (GSH) and superoxide dismutase (SOD) activities in addition to increased gene expression of apoptosis in benzo[α]pyrene-induced lung cancer[73].

Trigonelline is originally isolated from seeds of fenugreek or coffee and showed health benefits for several disorders[74]. Animals assigned for trigonelline treatment after the urethane treatment demonstrated a significant improvement in lung tumor volume and incidence. This finding could be attributed to the anti-invasive activity of trigonelline in cancer cells[75]. Trigonelline, on the contrary, significantly improved the bodyweight of urethane-treated mice. These findings are consistent with an earlier study that revealed trigonelline led to increased body weight by decreasing insulin resistance through activation of Peroxisome proliferator-activated receptor-γ/Glucose transporter type 4-leptin/ Tumor Necrosis Factor Alpha (PPAR-γ/GLUT4-leptin/TNF-α) signaling pathway[76]. Trigonelline exhibits antimitotic activity with a good prognosis in advanced NSCLC, indicated by a significant reduction of CYFRA 21-1[77]. IGF-1 is one of the autocrine products secreted by lung cancer cells with a poor prognosis. According to the research findings, trigonelline treatment urethane inhibits angiogenesis and is indicated by a significant reduction in IGF-1 levels. These effects may be attributed to the suppressive role of trigonelline on epidermal growth factor receptor (EGFR) and its impact on the IGF pathway[78,79].

Interestingly, trigonelline restored cGMP lung content in animals pretreated with urethane to normal value. Interestingly, trigonelline managed to restore cGMP lung content in urethane-treated mice to normal value. Trigonelline was found to have antioxidant and free radical scavenging properties, as well as a modulatory effect on both nitric oxides (NO) and inducible nitric oxide synthase (INOS)[80,81]. EGFR is inhibited by a cGMP-dependent protein kinase, which has potent apoptotic and antiproliferative activity in tumor cells[82].

Based on the study's findings, trigonelline promoted a programmed cell death for cancer cells that may be indicated by a significant reduction of anti-apoptotic biomarkers Bcl-2. The autophagic and apoptotic role of trigonelline in THP-1 cells may explain the inhibition of Bcl-2 expression[83].

Cyclin D1 plays an essential role in somatic cell growth in response to growth factors and

regulates G1-S transition[84]. In addition, cyclin D1 has been widely identified as an essential human oncogene[85]. Combined treatment with trigonelline and urethane showed a significant reduction in cyclin D1 expression that may be attributed to binding properties to cyclin-dependent kinase 4[86] novel phytoestrogen activity and stimulation of estrogen receptor (ER) expression at target gene[22,87]. The current study has proven the anti-angiogenic activity of trigonelline indicated by inhibition of Nrf2 expression. Qin et al[88] reported that the inhibitory action of trigonelline on Nrf2 transcription factors was associated with a reduction in cell cycle progression, which resulted in diminished cyclin D1 levels[89]. The antitumor effects of trigonelline can be attributed to its inhibitory action on Nrf2, which acts as tumor trigger[90]. This finding aligns with a previous study[91] that demonstrated that trigonelline reduces cell cycle progression through a significant delay of the G1/S boundary.

ICAM-1 has been expressed in several disorders like malignancies, asthma, and autoimmune disease and is induced by tumor necrosis factor-alpha (TNF-α), interleukin-1, and interferon-gamma. ICAM-1 has been expressed in several disorders like malignancies, asthma, and autoimmune disease and is induced by tumor necrosis factor-alpha (TNF-α), interleukin-1, and interferon-gamma. Trigonelline treatment showed a significant reduction of ICAM-1 level. This effect may be attributed to the direct inhibitory effects of trigonelline on TNF-α and IL-10 protein expression[76]. However, trigonelline exhibited antiangiogenic activity by direct inhibition of the MMP-2 level. The current study's data were aligned with earlier work that describes the MMP-2 level as a biomarker for cancer cell invasion and a prognostic indicator[92]. Moreover, the current study further explains the antiangiogenic activity of trigonelline that is indicated by a reduction of ICAM-1 and MMP-2 expressions, a remarkable inhibition of NF-kB, and downregulation of Bcl-2[58] and cyclin D1[59]. In the current study, the anti-inflammatory effect of trigonelline has been indicated by a marked inhibition of NF-κB p65 expression. NF-κB pathway also plays a crucial role in maintaining cell proliferation and invasion[56,61].

Trigonelline induced a substantial increase in active caspase 3 expressions due to its ability as a promotor for autophagic and apoptotic processes[83]. These results are compatible with a previous study that demonstrated trigonelline suppressed colon carcinogenesis through G1/S phase cell cycle arrest in mechanistic deduction of c-Myc expression and enhancement of caspase 3 activity[93]. Earlier studies[94] report the potential antitumor effects of trigonelline based on its role in EGFR inhibition in association with Nrf2 expression and translocation. It is well known that the EGFR pathway is a potential target for chemotherapy drug resistance[95]. Therefore, trigonelline expressed not only antitumor activity but also improved response to chemotherapy in NSCLC. Overall, these findings provide evidence on the biological antitumor effects of trigonelline through downregulation of cyclin D1, NF-κB, modulation of BAX/Bcl2 axis, and elevation of active caspase 3 expressions in addition to the reduction of Nrf2 expression with a remarked apoptosis[68]. In the present work, the histological analysis has proven that the results of biochemical and molecular investigations are consistent with prior studies[33,67].

Conclusions

It can be concluded that trigonelline outperforms conventional chemotherapy in terms of anticancer and apoptotic activity *via* multi-targets. It is also noteworthy that trigonelline appears to be a potential drug candidate for treating lung adenocarcinoma. Therefore, trigonelline should be involved in future studies to uncover its effect in overcoming the limitations of using chemotherapy.

Ethical Approval

The study was approved by the Ethics Committee of the Faculty of Pharmacy, Beni-Suef University (Permit Number: 018-43).

Acknowledgment

The authors are grateful to Prof. Mahmoud El-Begaway, Pathology Department, Faculty of Veterinary Medicine, Beni-Suef University for helping in pathological studies.
Sincere gratitude is offered to Dr. Demiana Samuel, Doctor of Audiology in USA, for her great help in editing this manuscript.

Conflict of Interest

The authors affirm that no conflict of interest.

Funding

This study was developed without external fundings.

Authors' Contributions

Writing the proposal, supervising during conduction of experiment, and performing data analysis: Mohamed A. Hamzawy.

Conducting experiment and writing manuscript: Marina N. Malak.

Writing study protocol and manuscript revision: Amira M. Abo-Youssef.

Participate in the design of the study protocol and supervision during experiment conduction, manuscript revision, and submission: Marwa M. Khalaf.

References

1) Fuentes N, Silva Rodriguez M, Silveyra P. Role of sex hormones in lung cancer. Exp Biol Med 2021; 246: 2098-2110.
2) Silveyra P, Fuentes N, Rodriguez Bauza DE. Sex and Gender Differences in Lung Disease. Adv Exp Med Biol 2021; 1304: 227-258.
3) Sung H, Ferlay J, Siegel RL, Laversanne M, Soerjomataram I, Jemal A, Bray F. Global cancer statistics 2020: GLOBOCAN estimates of incidence and mortality worldwide for 36 cancers in 185 countries. CA Cancer J Clin 2021; 71: 209-249.
4) Bray F, Ferlay J, Soerjomataram I, Siegel RL, Torre LA, Jemal A. Global Cancer Statistics 2018: GLOBOCAN Estimates of Incidence and Mortality Worldwide for 36 Cancers in 185 Countries. CA Cancer J Clin 2018; 68: 394-424.
5) Siegel RL, Miller KD, Fuchs HE, Jemal A. Cancer Statistics, 2021. CA Cancer J Clin 2021; 71: 7-33.
6) Torre LA, Siegel RL, Jemal A. Lung cancer statistics. Lung cancer and personalized medicine. Springer International Publishing, 2016.
7) Kulhánová I, Bray F, Fadhil I, Saeed AA, Elbasmy A, Anwar WA, Al-omari A, Shamseddine A, Znaor A, Soerjomataram I. Profile of cancer in the Eastern Mediterranean region: the need for action. Cancer Epidemiol 2017; 47: 125-132.
8) Abdelfattah S, El Wakeel H, Elghamry W, Ezzeldin M. 34P A retrospective analysis of the epidemiological and prognostic factors of non small cell lung cancer in an Egyptian tertiary referral center. J Thorac Oncol 2016; 11: S69-S70.
9) Bade BC, Cruz CSD. Lung cancer 2020: epidemiology, etiology, and prevention. Clin Chest Med 2020; 41: 1-24.
10) Dacic S. MTE02. 01 Update on WHO Classification and Staging of Lung Cancer. J Thorac Oncol 2018; 13: S207-S208.
11) Cheng L, Alexander RE, MacLennan GT, Cummings OW, Montironi R, Lopez-Beltran A, Cramer HM, Davidson DD, Zhang S. Molecular pathology of lung cancer: key to personalized medicine. Mod Pathol 2012; 25: 347-369.
12) Bernhardt EB, Jalal SI. lung cancer book 2016. Lung Cancer. Springer International Publishing, 2016.
13) Ardizzoni A, Boni L, Tiseo M, Fossella FV, Schiller JH, Paesmans M, Radosavljevic D, Paccagnella A, Zatloukal P,Mazzanti P, Bisset D, Rosell R. Cisplatin-versus carboplatin-based chemotherapy in first-line treatment of advanced non-small-cell lung cancer: an individual patient data meta-analysis. J Natl Cancer Inst 2007; 99: 847-857.
14) Halmos B, Burke T, Kalyvas C, Vandormael K, Frederickson A, Piperdi B. Pembrolizumab+ chemotherapy versus atezolizumab+ chemotherapy+/– bevacizumab for the first-line treatment of non-squamous NSCLC: A matching-adjusted indirect comparison. Lung Cancer 2021; 155: 175-182.
15) Oun R, Moussa YE, Wheate NJ. The side effects of platinum-based chemotherapy drugs: a review for chemists. Dalton Trans 2018; 47: 6645-6653.
16) Itoh K, Chiba T, Takahashi S, Ishii T, Igarashi K, Katoh Y, Oyake T, Hayashi N, Satoh K, Hatayama I, Yamamoto M, Nabeshima Y. An Nrf2/small Maf heterodimer mediates the induction of phase II detoxifying enzyme genes through antioxidant response elements. Biochem Biophys Res 1997; 236: 313-322.
17) Taguchi K, Motohashi H, Yamamoto M. Molecular mechanisms of the Keap1-Nrf2 pathway in stress response and cancer evolution. Genes Cells 2011; 16: 123-140.
18) Li J, Ichikawa T, Jin Y, Hofsethb LJ, Nagarkatti c P, Nagarkatti c M, Windust d A, Cui T. An essential role of Nrf2 in American ginseng-mediated anti-oxidative actions in cardiomyocytes. J Ethnopharmacol 2010; 130: 222-230.
19) Hayes JD, McMahon M. NRF2 and KEAP1 mutations: permanent activation of an adaptive response in cancer. Trends Biochem Sci 2009; 34: 176-188.
20) Jaramillo MC, Zhang DD. The emerging role of the Nrf2-Keap1 signaling pathway in cancer. Genes Dev 2013; 27: 2179-2191.
21) Milkovic L, Zarkovic N, Saso L. Controversy about pharmacological modulation of Nrf2 for cancer therapy. Redox Biol 2017; 12: 727-737.
22) Samatiwat P, Prawan A, Senggunprai L, Kukongviriyapan U, Kukongviriyapan V. Nrf2 inhibition sensitizes cholangiocarcinoma cells to cytotoxic and antiproliferative activities of chemotherapeutic agents. Tumor Biol 2016; 37: 11495-11507.
23) Zhu J, Wang H, Chen F, Fu J, Xu Y, Hou Y, Kou HH, Zhai C, Nelson MB, Zhang Q, Andersen ME, Pi J. An overview of chemical inhibitors of the Nrf2-ARE signaling pathway and their potential applications in cancer therapy. Free Radic Biol Med 2016; 99: 544-556.
24) Cano-Marquina A, Tarín J, Cano A. The impact of coffee on health. Maturitas 2013; 75: 7-21.

25) Banday AA, Lokhandwala MF. Oxidative stress impairs cGMP-dependent protein kinase activation and vasodilator-stimulated phosphoprotein serine-phosphorylation. Clin Exp Hypertens 2019; 41: 5-13.

26) Qiu Z, Wang K, Jiang C, Sua Y, Fana X, Lia J, Xuea S, Yao L. Trigonelline protects hippocampal neurons from oxygen-glucose deprivation-induced injury through activating the PI3K/Akt pathway. Chem Biol Interact 2020; 317: 108946-108952.

27) Arlt A, Sebens S, Krebs S, Geismann C , Grossmann M , Kruse ML , Schreiber S, Schäfer H. Inhibition of the Nrf2 transcription factor by the alkaloid trigonelline renders pancreatic cancer cells more susceptible to apoptosis through decreased proteasomal gene expression and proteasome activity. Oncogene 2013; 32: 4825-4835.

28) Jeong YI, Kim DH, Chung KD, Kim YH, Lee YS, Choi K-C. Antitumor activity of trigonelline-incorporated chitosan nanoparticles. J Nanosci Nanotechnol 2014; 14: 5633-5637.

29) Tazehkand AP, Salehi R, Velaei K, Samadi N. The potential impact of trigonelline loaded micelles on Nrf2 suppression to overcome oxaliplatin resistance in colon cancer cells. Mol Biol Rep 2020; 47: 5817-5829.

30) Roh JL, Jang H, Kim EH, Shin D. Targeting of the glutathione, thioredoxin, and Nrf2 antioxidant systems in head and neck cancer. Antioxid Redox Signal 2017; 27: 106-114.

31) Roh JL, Kim EH, Jang H, Shin D. Nrf2 inhibition reverses the resistance of cisplatin-resistant head and neck cancer cells to artesunate-induced ferroptosis. Redox Biol 2017; 11: 254-262.

32) Fath M, Ahmad IM, Smith CJ, Spence JM, Spitz DR. Enhancement of carboplatin-mediated lung cancer cell killing by simultaneous disruption of glutathione and thioredoxin metabolism. Clin Cancer Res 2011; 17: 6206-6217.

33) Hamzawy MA, Abo-youssef AM, Salem HF, Mohammed SA. Antitumor activity of intratracheal inhalation of temozolomide (TMZ) loaded into gold nanoparticles and/or liposomes against urethane-induced lung cancer in BALB/c mice. Int J Drug Deliv 2017; 24: 599-607.

34) Hamzawy M, Abo-youssef A, Salem H, Sameh Mohamed A. An Additional risk of Lung Cancer from Recurrent Exposure to Ethyl Carbamate (EC) in BALB/C Mice. J Cancer Sci Ther. 2015; 7: 359-362.

35) Jensen MM, Jørgensen JT, Binderup T, Kjær A. Tumor volume in subcutaneous mouse xenografts measured by microCT is more accurate and reproducible than determined by 18 F-FDG-microPET or external caliper. BMC medical imaging 2008; 8: 1-9.

36) Rodriguez PL, Harada T, Christian DA, Pantano DA, Tsai RK, Discher DE. Minimal" Self" peptides that inhibit phagocytic clearance and enhance delivery of nanoparticles. Science 2013; 339: 971-975.

37) Stieber P, Hasholzner U, Bodenmüller H, Nagel D, Sunder-Plassmann L, Dienemann H, Meier W, Fateh-Moghadam A. CYFRA 21-1: A new marker in lung cancer. Cancer 1993; 72: 707-713.

38) Fu L, Wang R, Yin L, Shang X, Zhang R, Zhang P. CYFRA21-1 tests in the diagnosis of non-small cell lung cancer: a meta-analysis. Int J Biol Markers 2019; 34: 251-261.

39) Su JL, Stimpson S, Edwards C, Van Arnold J, Burgess S, Lin P. Neutralizing IGF-1 monoclonal antibody with cross-species reactivity. Hybridoma 1997; 16: 513-518.

40) Chi Xx, Zhang T, Chu Xl. Effect of genistein on IGF-1 and IGFBP-1 in young and aged female rat ovary. J Anim Physiol Anim Nutr 2019; 103: 1594-1601.

41) Ferrini MG, Garcia E, Abraham A, Artaza JN, Nguyen S, Rajfer J. Effect of ginger, Paullinia cupana, muira puama and L-citrulline, singly or in combination, on modulation of the inducible nitric oxide-NO-cGMP pathway in rat penile smooth muscle cells. Nitric Oxide. 2018; 76: 81-86.

42) Wang Z, Guo Z, Song T, Zhang X, He N, Liu P, Wang P, Zhang Z. Proteome-Wide Identification of On-and Off-Targets of Bcl-2 Inhibitors in Native Biological Systems by Using Affinity-Based Probes (AfBPs). ChemBioChem 2018; 19: 2312-2320.

43) Wu Y, Zou D, Cao Y, Yao N, Wang J, Wang W, Jiang H, Li G. Expression and purification of a human anti-cyclin D1 single-chain variable fragment antibody AD5 and its characterization. Int J Mol Med 2013; 32: 1451-1457.

44) Pattamapun K, Handagoon S, Sastraruji T, Gutmann JL, Pavasant P, Krisanaprakornkit S. Decreased levels of matrix metalloproteinase-2 in root-canal exudates during root canal treatment. Arch Oral Biol 2017; 82: 27-32.

45) Yang J, Tian H, Huang X. Tephrosin attenuates sepsis induced acute lung injury in rats by impeding expression of ICAM-1 and MIP-2. Microb Pathog 2018; 117: 93-99.

46) Bancroft JD, Gamble M. Theory and practice of histological techniques. Elsevier Health Sciences, 2008.

47) Curtis MJ, Alexander S, Cirino G, Docherty JR, George CH, Giembycz MA, Hoyer D, Insel PA, Izzo AA, Ji Y, MacEwan DJ, Sobey CG, Stanford SC, Teixeira MM, Wonnacott S, Ahluwalia A. Experimental design and analysis and their reporting II: updated and simplified guidance for authors and peer reviewers. Br J Pharmacol 2018; 175: 987-993.

48) Snedecor GW, Cochran WG. Statistical methods, 8thEdn. Ames: Iowa State Univ Press Iowa, 1989.

49) Chen RJ, Tsai SJ, Ho CT, Pan MH, Ho YH, Wu CH, Wang YJ. Chemopreventive effects of pterostilbene on urethane-induced lung carcinogenesis in mice via the inhibition of EGFR-mediated pathways and the induction of apoptosis and autophagy. J Agric Food Chem 2012; 60: 11533-11541.

50) Gurley KE, Moser RD, Kemp CJ. Induction of lung tumors in mice with urethane. Cold Spring Harbor Protocols, 2015.

51) Dall'Olio FG, Abbati F, Facchinetti F, Massucci M, Melotti B, Squadrilli A, Buti S, Formica F, Tiseo M, Ardizzoni A. CEA and CYFRA 21-1 as prognostic biomarker and as a tool for treatment monitoring in advanced NSCLC treated with immune checkpoint inhibitors. Ther Adv Med Oncol 2020; 12: 1-13.

52) Tas F, Bilgin E, Tastekin D, Erturk K, Duranyildiz D. Serum IGF-1 and IGFBP-3 levels as clinical markers for patients with lung cancer. Biomed Rep 2016; 4: 609-614.

53) Kotsantis I, Economopoulou P, Psyrri A, Maratou E, Pectasides D, Gogas H, Kentepozidis N, Mountzios G, Dimitriadis G, Giannouli S. Prognostic significance of IGF-1 signalling pathway in patients with advanced non-small cell lung cancer. Anticancer Res 2019; 39: 4185-4190.

54) Jiang W, Meng L, Xu G, Lv C, Wang H , Tian H , Chen R , Jiao B, Wang B, Huang C. Wentilactone A induces cell apoptosis by targeting AKR1C1 gene via the IGF 1R/IRS1/PI3K/AKT/Nrf2/FLIP/Caspase 3 signaling pathway in small cell lung cancer. Oncol Lett 2018; 16: 6445-6457.

55) Tang H, Liao Y, Xu L, Zhang C, Liu Z, Deng Y, Jiang Z, Fu S, Chen Z, Zhou S. Estrogen and insulin-like growth factor 1 synergistically promote the development of lung adenocarcinoma in mice. Int J Cancer 2013; 133: 2473-2482.

56) Hoesel B, Schmid JA. The complexity of NF-κB signaling in inflammation and cancer. Mol Cancer 2013; 12: 86-101.

57) Stathopoulos GT, Sherrill TP, Cheng DS, Scoggins RM, Han W, Polosukhin VV, Connelly L, Yull FE, Fingleton B, Blackwell TS. Epithelial NF-κB activation promotes urethane-induced lung carcinogenesis. Proc Natl Acad Sci 2007; 104: 18514-18519.

58) Bharti AC, Aggarwal BB. Nuclear factor-kappa B and cancer: its role in prevention and therapy. Biochem Pharmacol 2002; 64: 883-888.

59) Chen W, Li Z, Bai L, Lin Y. NF-kappaB, a mediator for lung carcinogenesis and a target for lung cancer prevention and therapy. Front Biosci 2011; 16: 1172-1185.

60) Willis A, Sabeh F, Li XY and Weiss S. Extracellular matrix determinants and the regulation of cancer cell invasion stratagems. J Microsc 2013; 251: 250-260.

61) Kotteas EA, Boulas P, Gkiozos I, Tsagkouli S, Tsoukalas G, Syrigos KN. The intercellular cell adhesion molecule-1 (icam-1) in lung cancer: implications for disease progression and prognosis. Anticancer Res 2014; 34: 4665-4672.

62) Creagh EM. Caspase crosstalk: integration of apoptotic and innate immune signalling pathways. Trends Immunol 2014; 35: 631-640.

63) Zahran MH, Hussein AM, Barakat N, Awadalla A, Khater S, Harraz A, Shokeir AA. Sildenafil activates antioxidant and antiapoptotic genes and inhibits proinflammatory cytokine genes in a rat model of renal ischemia/reperfusion injury. Int Urol Nephrol 2015; 47: 1907-1915.

64) Wu SH, Hsiao YT, Kuo CL, Yu FS, Hsu SC, Wu PP, Chen JC, Hsia TC, Liu HC, Hsu WH, Chung JG. Bufalin inhibits NCI-H460 human lung cancer cell metastasis in vitro by inhibiting MAPKs, MMPs, and NF-κB pathways. Am J Chinese Med 2015; 43: 1247-1264.

65) Bauer AK, Cho HY, Miller-DeGraff L, Walker C, Helms K, Fostel J, Yamamoto M, Kleeberger SR. Targeted deletion of Nrf2 reduces urethane-induced lung tumor development in mice. PLoS One 2011; 6: e26590-e26605.

66) Satoh H, Moriguchi T, Takai J, Ebina M, Yamamoto M. Nrf2 prevents initiation but accelerates progression through the Kras signaling pathway during lung carcinogenesis. Cancer Res 2013; 73: 4158-4168.

67) Mishra M, Jiang H, Chawsheen HA, Gerard M, Toledano MB, Wei Q. Nrf2-activated expression of sulfiredoxin contributes to urethane-induced lung tumorigenesis. Cancer Lett 2018; 432: 216-226.

68) Tong YH, Zhang B, Fan Y, Lin NM. Keap1-Nrf2 pathway: A promising target towards lung cancer prevention and therapeutics. Chron Diseases Translat Med 2015; 1: 175-186.

69) Menegon S, Columbano A, Giordano S. The dual roles of NRF2 in cancer. Trends Mol Med 2016; 22: 578-593.

70) Ho GY, Woodward N, Coward JI. Cisplatin versus carboplatin: comparative review of therapeutic management in solid malignancies. Crit Rev Oncol Hematol 2016; 102: 37-46.

71) Wang D, Lippard SJ. Cellular processing of platinum anticancer drugs. Nat Rev Drug Discov 2005; 4: 307-320.

72) Griesinger F, Korol EE, Kayaniyil S, Varol N, Ebner T, Goring SM. Efficacy and safety of first-line carboplatin-versus cisplatin-based chemotherapy for non-small cell lung cancer: A meta-analysis. Lung Cancer. 2019; 135: 196-204.

73) Lee HY, Kim IK, Lee HI, Lee HY, Kang HS, Yeo CD, Kang HH, Moon HS, Lee HS. Combination of carboplatin and intermittent normobaric hyperoxia synergistically suppresses benzo [a] pyrene-induced lung cancer. Korean J Intern Med 2018; 33: 541-551.

74) Khalili M, Alavi M, Esmaeil-Jamaat E, Baluchnejadmojarad T, Roghani M. Trigonelline mitigates lipopolysaccharide-induced learning and memory impairment in the rat due to its anti-oxidative and anti-inflammatory effect. Int Immunopharmacol 2018; 61: 355-362.

75) Hirakawa N, Okauchi R, Miura Y, Yagasaki K. Anti-invasive activity of niacin and trigonelline against cancer cells. Biosci Biotechnol Bioch 2005; 69: 653-658.

76) Li Y, Li Q, Wang C, Lou Z, Li Q. Trigonelline reduced diabetic nephropathy and insulin resistance in type 2 diabetic rats through peroxisome proliferator activated receptor γ. Exp Ther Med 2019; 18: 1331-1337.

77) Yoshimura A, Uchino J, Hasegawa K, Tsuji T, Shiotsu S, Yuba T, Takumi C, Yamada T, Takayama K, Hiraoka N. Carcinoembryonic antigen and CYFRA 21-1 responses as prognostic factors in advanced non-small cell lung cancer. Transl Lung Cancer Res 2019; 8: 227-234.

78) Pillai RN, Ramalingam SS. Inhibition of insulin-like growth factor receptor: end of a targeted therapy? Transl Lung Cancer Res 2013; 2: 14-22.

79) Fouzder C, Mukhuty A, Mukherjee S, Malick C, Kundu R. Trigonelline inhibits Nrf2 via EGFR signalling pathway and augments efficacy of Cisplatin and Etoposide in NSCLC cells. Toxicol In Vitro 2021; 70: 105038-105047.

80) Zhou J, Zhou S, Zeng S. Experimental diabetes treated with trigonelline: effect on β cell and pancreatic oxidative parameters. Fundam Clin Pharmacol 2013; 27: 279-287.

81) Lorigooini Z, Dehsahraei KS, Bijad E, Dehkordi SH, Amini-Khoei H. Trigonelline through the attenuation of oxidative stress exerts antidepressant-and anxiolytic-like effects in a mouse model of maternal separation stress. Pharmacology 2020; 105: 289-299.

82) Li D, Hua Y, Jiang L, Huang Y, Yue J, Wu Y, Chen Y. Cyclic Guanosine Monophosphate (cGMP)-Dependent Protein Kinase II Blocks Epidermal Growth Factor (EGF)/Epidermal Growth Factor Receptor (EGFR)-Induced Biological Effects on Osteosarcoma Cells. Int j exp clin res 2018; 24: 1997-2002.

83) Akın D, Berk SC, Şener YA, Kepenek AO, Özdaş ŞB, Demircan G. Trigonelline's effect on BCL-2 protein expression level in THP-1 cells. J Biotechnol 2019; 305: s21-s32.

84) Tchakarska G, Sola B. The double dealing of cyclin D1. Cell Cycle 2020; 19: 163-178.

85) Tashiro E, Tsuchiya A, Imoto M. Functions of cyclin D1 as an oncogene and regulation of cyclin D1 expression. Cancer Sci 2007; 98: 629-635.

86) Aladi EO, Hadiza RJ, Opeyemi EG, Joseph OA, Iyanuoluwa OE, Samuel AN, Damilohun MS, Idowu OO. Molecular binding signatures of Trigonella foenum-graecum compounds on cyclin-dependent kinase 4 for possible anti-cancer mechanism in breast cancer. GSC biol pharm sci 2020; 11: 014-021.

87) Allred KF, Yackley KM, Vanamala J, Allred CD. Trigonelline is a novel phytoestrogen in coffee beans. J Nutr 2009; 139: 1833-1838.

88) Qin W, Guan D, Ma R, Yang R, Xing G, Shi H, Tang G, Li J, Lv H, Jiang Y. Effects of trigonelline inhibition of the Nrf2 transcription factor in vitro on Echinococcus granulosus. Acta Biochim Biophys 2017; 49: 696-705.

89) Lin Y, Sui LC, Wu RH, MA RJ, FU HY, XU JJ, QIU XH, CHEN L. Nrf2 inhibition affects cell cycle progression during early mouse embryo development. J Reprod Dev 2018; 64: 49-55.

90) Sánchez-Ortega M, Carrera AC, Garrido A. Role of NRF2 in Lung Cancer. Cells. 2021; 10: 1879-1907.

91) Sathiyaseelan A, Saravanakumar K, Jayalakshmi J, Gopi J, Shajahan A, Barathikannan K, Kalaichelvan PT, Wang MH. Trigonelline-loaded chitosan nanoparticles prompted antitumor activity on glioma cells and biocompatibility with pheochromocytoma cells. Int J Biol Macromol 2020; 163: 36-43.

92) Reich R, Supuran CT, Breuer E. Tumor microenvironment as target in cancer therapy. Annu Rep Med Chem 2014; 49: 269-284.

93) Yoo G, Allred CD. The estrogenic effect of trigonelline and 3, 3-diindolymethane on cell growth in non-malignant colonocytes. Food Chem Toxicol 2016; 87: 23-30.

94) Fouzder C, Mukhuty A, Mukherjee S, Malick C, Kundu R. Trigonelline inhibits Nrf2 via EGFR signalling pathway and augments efficacy of Cisplatin and Etoposide in NSCLC cells. Toxicol In Vitro 2021; 70: 105038-105047.

95) Leonetti A, Assaraf YG, Veltsista PD, El Hassouni B, Tiseo M, Giovannetti E. MicroRNAs as a drug resistance mechanism to targeted therapies in EGFR-mutated NSCLC: Current implications and future directions. Drug Resist Updat 2019; 42: 1-11.